# The Local Volume Legacy Survey


**Principal Investigator:** Robert C. Kennicutt

**Institution:** University of Cambridge and University of Arizona

**Electronic mail:** robk@ast.cam.ac.uk

**Technical Contact:** Charles W. Engelbracht, University of Arizona

**Co−Investigators:** Ayesha Begum, University of Cambridge
Daniela Calzetti, University of Massachusetts
Julianne Dalcanton, University of Washington
Danny Dale, University of Wyoming
Charles Engelbracht, University of Arizona
Jose Funes, Vatican Observatory
Amando Gil de Paz, University of Madrid
Karl Gordon, University of Arizona
Benjamin Johnson, Columbia University
Janice Lee, NOAO/Carnegie
Shoko Sakai, UCLA
Evan Skillman, University of Minnesota
Liese van Zee, Indiana University
Fabian Walter, MPIA
Daniel Weisz, University of Minnesota
Benjamin Williams, University of Washington
Yanling Wu, Cornell University


**Science Category:** Extragalactic: nearby galaxies (z<0.05, v_sys<15,000 km/s)

**Hours Requested:** 280.5

**Proprietary Period(days):** 0


**Abstract:**
The Local Volume Legacy (LVL) is an IRAC and MIPS survey of a volume−complete sample of 258 galaxies within the 11 Mpc local volume. Its broad goal is to provide critical insight into two of the primary processes that shape the growth of galaxies: star formation and its interaction with the interstellar medium. This goal will be accomplished by investigating the spatially−resolved star formation, dust, and red stellar populations of local galaxies which

span the full diversity of luminosities, surface brightnesses, metallicities, dust properties, and star formation properties. The survey will also provide an infrared and multi−wavelength census of the Galactic neighborhood, exploiting the highest spatial resolution and absolute depth achievable with Spitzer. LVL is unique in that it extends current Spitzer observations of galaxies to an unbiased, fully representative, and statistically robust sample of nearby galaxies. The tiered survey includes: (1) all known galaxies inside a sub−volume bounded by 3.5 Mpc (HST ANGST Treasury survey), and (2) an unbiased sample of S−Irr galaxies within the larger, and more representative, 11 Mpc sphere (GALEX 11HUGS survey). Our strategy provides volume−complete coverage of galaxies over the entire luminosity function, with the minimum sample needed to fully characterize the local galaxy population. The Spitzer observations will leverage a rich suite of multi−wavelength ancillary data from the ANGST and 11HUGS surveys, including H−alpha and GALEX UV imaging, stellar population mapping with HST, HI mapping with the VLA and GMRT, and broad−band optical imaging and spectroscopy, to enhance the scientific return and provide an enduring core dataset on the Galactic neighborhood for the scientific community at large.

# 1 Scientific Justification

## 1.1 Introduction: The Local Volume Legacy

The study of galactic evolution has matured enormously over the past 15 years, producing a paradigm which integrates the theory of galaxy formation and evolution with the larger theory of cosmology and structure formation. However, while the broad outlines of galaxy evolution have taken shape, the details have yet to be filled in. Our understanding of the actual physical processes that shape the growth of galaxies – most notably star formation and its interaction with the ISM – are acutely limited.

Spitzer has the power to provide critical insight into these mechanisms, via its ability to (1) probe the component of the UV and optical light that is reprocessed into the infrared; (2) characterize the physical state of the dusty ISM; and (3) map the structure of the old, red stellar populations. Spitzer observations already have begun to achieve this objective, thanks to the Spitzer Infrared Nearby Galaxies Survey (SINGS; Kennicutt et al. 2003) and other GO and GTO programs. However, as illustrated in Figures 1 & 2, these Spitzer studies are incomplete, and show the common observational bias toward massive, metal-rich, and high surface brightness galaxies. The sampling that does exist for lower mass systems is sparse, and is far from representative, despite the fact that this population offers the greatest diversity of properties, the best-measured star formation histories, and hence optimal leverage for elucidating the processes that underlie star formation and shape the properties of galaxies. Gaining this leverage depends on (1) maximizing the range of metallicities, masses, star formation rates and histories, and dust contents in a given sample, and (2) gaining access to a large and representative number of galaxies, to provide the statistical power needed to separate dependencies among multiple variables.

Luckily, ideal samples which meet these requirements now exist. Superb, *volume-limited* studies of galaxies, in particular the 11 Mpc H$\alpha$ Ultraviolet Galaxy Survey (11HUGS) and ACS Nearby Galaxy Survey Treasury (ANGST) programs, provide robust datasets for probing the properties of star formation and the ISM. The galaxies in these samples span the full ranges of star formation modes and host galaxy properties, and provide a complete and statistically unbiased view of the Local Volume population. Moreover, the galaxies, being among our nearest neighbors, offer the best spatial resolution and faintest absolute detection limits possible. The 11HUGS and ANGST surveys also supply a rich suite of multi-wavelength data including H$\alpha$ and GALEX UV imaging, stellar population mapping with HST, HI mapping with the VLA and the GMRT, and broad-band optical and NIR imaging. *Spitzer observations would complete the full SED coverage for these galaxies, and finally secure a true Legacy dataset for the Local Volume.*

With the *Local Volume Legacy* we propose to complete IRAC and MIPS observations of 258 galaxies from the combined 11HUGS and ANGST surveys. To maximize the coverage of galaxy properties and science return per hour of observing time, we employ a tiered survey strategy (Fig. 3) including (1) *all* known galaxies inside a sub-volume bounded by $\sim$3.5 Mpc, and (2) an unbiased set of late-type galaxies within the larger, and more representative, 11 Mpc sphere. The resultant sample will provide a comprehensive and statistically robust characterization of star formation activity and ISM properties in the Local Volume population based on UV-to-IR SED maps, with the minimum sample needed to achieve this objective. As befitting for a Legacy program, we will deliver an integrated, homogeneously processed multi-wavelength data archive (including the new data along with reprocessed archival observations), produced to the high standards of the SINGS project.

## 1.2 Science Goals: Demographics of Stars and Dust in Galaxies

The multi-wavelength UV-to-FIR SED census provided by the *Local Volume Legacy (LVL)* will be the definitive core dataset on the Galactic neighborhood for at least the next decade, and will enable the community to make progress on a wide range of astrophysical problems. Here, we outline some of the principal science issues to be addressed by our team, with emphasis on those that exploit the unique properties of a volume-limited dataset.

• FIR Emission and Dust in Galaxies Across the Luminosity Function

The proposed MIPS observations of the *LVL* sample will provide the first truly comprehensive local inventory of the dusty ISM in galaxies over the entire luminosity function. As shown in the bottom panel of Figure 1, our knowledge of even the integrated infrared properties of galaxies is mainly limited to luminous galaxies ($M_B < -17$); the inventory of IRAS measurements for fainter systems and brighter early-type galaxies is dominated by nondetections. SINGS and a few other Spitzer programs have extended this knowledge to a handful of low-mass galaxies, but the sampling is severely limited (Dale et al. 2005, 2007). *LVL* will break new ground with a full characterization of the population, and significantly advance our understanding of the dust contents and FIR SEDs of low-mass galaxies.

These limited available observations show that dust emission is not connected in any simple way to galaxy mass, gas content, or metallicity (e.g., Dale et al. 2007, Walter et al. 2007). For example the second most metal-poor dIrr galaxy known, SBS0335-052, has an infrared luminosity of more than $10^9$ $L_\odot$ and embedded super star clusters with visual extinctions of at least 12 mag (e.g., Houck et al. 2004). Given that the dependence of dust content on metallicity and gas mass is non-trivial, the other factors controlling the dust-to-gas ratio must be identified. To do so, we will characterize the infrared SEDs, warm dust masses, and temperature distributions across the extensive range of physical conditions covered by our local sample, and identify the processes that drive changes in the dust-to-gas ratio. This work will benefit from high-resolution HI maps available or being obtained with the VLA, GMRT, and ACTA for more than 100 of our galaxies.

Beyond constructing integrated galaxy SEDs, the proximity of the *LVL* sample allows us to create spatially-resolved maps of the dust mass and total SFR. The resulting maps offer the best opportunity outside the Local Group to cleanly separate individual dusty regions, many of which will have local star formation histories measured from color-magnitude diagrams (CMDs) constructed from HST imaging. These maps will also constrain the physical nature of the dust heating in galaxies, and the lifetimes of the heating populations in particular. By correlating the ages of the underlying stellar populations (from ANGST) with the observed infrared emission, we can empirically calibrate the duration over which FIR emission is detectable. These measurements can be made for hundreds of different regions within the sample galaxies, for a wide variety of metallicities and starburst amplitudes.

• PAH Emission and Star Formation in Galaxies

Emission from small "PAH" molecules/grains dominates the mid-infrared radiation of most nearby galaxies, and has become a primary SFR indicator for high-redshift dusty galaxies (e.g., Daddi et al. 2005, Pérez-González et al. 2005, Yan et al. 2005, Valiante et al. 2007). Understanding the physical factors that influence the strength of the PAH emission, and establishing its reliability as a SFR tracer is thus of paramount importance. ISO and Spitzer have shown that PAH emission is generally well-correlated with independent measures of the SFR in luminous and metal-rich galaxies (e.g., Roussel et al. 2001, Förster-Schreiber et al. 2004, Dale et al. 2005, 2007), but weakens or disappears altogether in galaxies with metallicities below 0.3–0.5 solar (e.g., Engelbracht et al. 2005, Rosenberg et al. 2006, Wu et al. 2006). However, other factors such as the strength and hardness of the local radiation field also influence the PAH band strengths (Madden et al. 2006 and references above). Separating these effects has proven difficult, due to limited numbers of observations and a strong bias toward compact starburst galaxies.

Our IRAC imaging will make significant inroads to this important problem. Our sample spans the metallicity range over which the PAH emission changes, and covers large dynamic ranges ($10^5$) in the total SFR, the SFR/area, and the UV-radiation intensity. Our proposed observations will include sufficient numbers of galaxies to separate the effects of metallicity, the hardness of the radiation field, and the star formation rate. Specifically, we will use the IRAC 8.0 $\mu$m, IRAC 4.5 $\mu$m, and MIPS 24 $\mu$m images to generate continuum-subtracted maps of the 7.7 $\mu$m PAH emission. We will compare these spatially well-resolved maps to the local strength and hardness of the background UV radiation field (as measured from our GALEX, H$\alpha$, and HST imaging) and with metallicity (as measured from optical spectra). We are well aware from our experience with SINGS and the MIPS and IRS GTO projects that continuum-subtracted 8 $\mu$m band maps are no substitute for spectra, and need to be interpreted conservatively when the PAH emission is weak. However with proper allowance for uncertainties these data will significantly increase the available constraints on PAH emission strengths in unusual environments, and complement the many ongoing spectroscopic studies of PAH emission in galaxies.

• Diagnostics and Demographics of Star Formation and Starbursts

The inventory of UV-to-FIR SEDs produced by the *Local Volume Legacy* capture essential information about the star formation rate (SFR). The *combination* of UV, H$\alpha$, and infrared observations encompasses all the light emitted by short-lived massive stars; the first two of these components trace light emitted by O & B stars, whereas the FIR luminosity captures the light that is absorbed and re-radiated by dust. We will use these SED's to derive accurate *spatially-resolved* SFRs that are independent of extinction (which can be substantial even in low-luminosity galaxies; e.g., Houck et al. 2004, Cannon et al. 2005; 2006a, b). The SINGS project has used this technique to calibrate extinction-corrected SFR indices for HII regions and galaxies (e.g. Calzetti et al. 2005; Kennicutt et al. 2007a, b). The resulting star formation rates are vastly superior to the constant-factor extinction corrections that have traditionally been applied to H$\alpha$ and UV-based SFRs (Kennicutt 1998).

These data offer the opportunity to complete this calibration of the suite of SFR diagnostics (UV continuum, H$\alpha$, 8 $\mu$m emission, 24 $\mu$m and FIR continuum, radio continuum) initiated by SINGS and previous programs, over the complete range of host galaxy metallicities and star formation properties. A full understanding of the dependences of the zeropoints, scatter, and systematic errors of these methods is critical, if we are to apply these SFR and extinction estimators to high-redshift objects, whose metallicities, physical conditions, and star formation modes can differ markedly from those at the present day.

A second major program will assess the demographics of star formation and starbursts in the local galaxy population. First, we will construct and analyze volume-averaged UV-to-FIR SEDs of star-forming galaxies as a function of mass, SFR, and morphological type. Second, we will use the distribution of SFRs to calculate the frequencies of starbursts in a given mass range, providing a direct measurement of the duty cycle. We have performed an initial duty cycle analysis using the H$\alpha$ data from 11HUGS (Lee 2006), but major uncertainties remain due to the lack of complete extinction information. These undertakings demand the *LVL* unbiased, complete sample – they are simply impossible with datasets such as SINGS alone, which contain a physically diverse but non-representative sampling of galaxies, rather than all star-forming galaxies in a given volume. Finally, we will produce a spatially resolved temporal characterization of the different modes of star formation (e.g., bursts *vs* continuous) by exploiting the range of timescales for different SFR tracers, such as the emission from the FUV, NUV and optical recombination lines. Dust extinction strongly biases each of these tracers, so observations of the re-radiated light in the mid- and far-infrared are crucial.

• Stellar Structure and Populations of Dwarf Galaxies

Infrared starlight is a critical probe of the underlying stellar mass of a galaxy. At IRAC's 3.6 and 4.5 $\mu$m wavelengths, galaxies are dominated by a scattering of bright AGB stars and M supergiants, superimposed on a diffuse sheet of red giant branch stars (Cannon et al. 2006). These smoothly distributed older stellar populations are one of the most robust tracers of the stellar mass of the galaxy, but they are largely undetectable from the ground for galaxies with low masses and low surface brightnesses. What little near-infrared imaging has been done has been directed at Local Group galaxies or blue compact starburst galaxies (e.g., Noeske et al. 2005 and references therein).

*LVL* will bring the unparalleled infrared surface brightness sensitivity of IRAC to bear on measuring the stellar masses of a truly unbiased set of the nearest galaxies. Thanks to the reduced IR sky from space, our imaging strategy produces S/N ratios of >10 at the optical ($R_{25}$) radii of the disks, far beyond the radius where NIR observations are effective from the ground. We will use 3.6 and 4.5 $\mu$m imaging to map the locations of AGB and M-supergiants, and to trace the spatial distribution of underlying stellar mass. These stellar masses will be an important parameter in the dust and star formation studies discussed above, and their spatial distribution will provide essential information about the background density field in which the interaction between star formation and the ISM is taking place. In addition, we will use the subset of the sample with resolved stellar populations from HST to calibrate the relationship between IRAC colors and luminosities and the star formation history and metallicity of the underlying stellar populations. Only the *LVL* sample is sufficiently large, close, and diverse to provide the foundation of data necessary for such a calibration.

## 1.3 Summary and Legacy Value

As we enter Spitzer's final 2 years of full operations, it is essential that we identify vital pieces missing from the foundation of infrared data upon which we will rely for the next decade and beyond. Figures 1 & 2 demonstrate a compelling need for improved Spitzer coverage of our Local Volume, with current observations being far from representative of the population as a whole. These observations of our nearest neighbors will provide data with exquisite spatial resolution and depth, and with coverage that is not merely representative, but also true to the statistics rendered by a volume-complete sample. Building on our experience and successes with SINGS, the *Local Volume Legacy* survey will fill the remaining fundamental gap in our knowledge of the infrared properties of the local population. The added value provided by the unprecedented investment of existing Spitzer, GALEX, HST, VLA, ground-based imaging & spectroscopy (and planned observations with Herschel for *LVL* galaxies) assures a rich scientific return on the Spitzer time investment. Our unique combination of multi-wavelength observations of the gas, stars and dust in an optimally selected sample of Local Volume galaxies, and the scientific and technical expertise of our team, will not only yield new insights into the mechanisms that drive, regulate and extinguish star-formation, but also supply a enduring core dataset on the Galactic neighborhood for the scientific community at large.

# 2 Technical Plan

## 2.1 Sample Definition and Justification

The *Local Volume Legacy* aims to provide a comprehensive and statistically robust characterization of the star formation activity and ISM properties of galaxies based on a UV-to-IR census of our nearest galactic neighbors. We employ a tiered "wedding cake" strategy (Figure 3) which consolidates the complementary strengths of two existing volume-limited studies, the ACS Nearby Galaxy Survey Treasury (ANGST; PI Dalcanton) program and the 11 Mpc H$\alpha$ UV Galaxy Survey (11HUGS; PI Kennicutt).

The inner tier of *LVL* is anchored by the ANGST sample. It includes *all* 69 known galaxies outside of the Local Group within $D < 3.5$ Mpc and $|b| > 20°$, with an extension to $\sim$4 Mpc in the direction of the M81 group. This volume includes spiral, dIrr, dSph, and tidal dwarf galaxies, spanning a range of 6 magnitudes in luminosity, $10^3$ in current SFR, and 1.5 dex in metallicity. The survey augments existing deep HST imaging with new observations, and provides complete stellar photometry with homogeneous depth. The resulting CMDs allow us to reconstruct maps of the galaxies' star formation histories over the last 500 Myrs, with a time resolution as short as 30 Myrs (e.g. Dohm-Palmer et al. 1997). Most ANGST galaxies are in 11HUGS, and GALEX UV and H$\alpha$ observations for the faintest remaining galaxies are being obtained. In addition, a $\sim$500 hr VLA program has recently been awarded for B, C, & D array mapping of the sample. HST data are in hand for 58 of the 72 galaxies now, and the ANGST team is engaged in overcoming the challenge presented by the recent failure of ACS, using a WFPC2 and WFC3 observations.

The outer tier of *LVL* is drawn from 11HUGS, which began as an H$\alpha$+broadband imaging study of a volume-limited sample of 400 spiral and irregular galaxies within 11 Mpc. The survey was expanded to include GALEX UV observations for 220 galaxies with $|b| \geq 30°$ and $B < 15.5$. Statistical tests and comparisons with blind all-sky HI surveys (Ryan-Weber et al. 2002, Lee 2006) show that the catalog completeness for S-Irr galaxies out to 11 Mpc is excellent (>95%) within limits of $|b| \geq 20°$, and $B \leq 15.5$. We optimize our proposed Spitzer observations of 11HUGS galaxies by restricting the sample to where we have high completeness and multi-wavelength coverage, and imposing limits of $B \leq 15.5$ and $|b| \geq 30°$.

These conjoined surveys are highly complementary, with ANGST providing complete coverage within its volume including all galaxy types and complete coverage of the very lowest mass galaxies, while 11HUGS covers a 30× larger survey volume, and thereby offers a more complete and more representative sampling of the star-forming galaxy population as a whole (10 magnitudes range in luminosity, $10^5$ in SFR, and 2 dex in metallicity). This sampling is especially critical for capturing a complete range of star formation modes in the low-mass galaxies (burst, post-burst, and quiescient modes at different surface brightnesses) and to ensure full and unbiased sampling of the more massive galaxies (only a handful are contained in the ANGST volume). However we do not need to observe the entire 435 galaxy ANGST+11HUGS sample to accomplish these objectives. Instead, optimal statistical sampling can be achieved with 2-3 galaxies per 1 magnitude cell in two-parameter plots of $M_B$, $L_{IR}/L_B$, SFR/mass, and SFR/area (see Figures 1–2). Since the galaxies in Figure 1 span approximately 10 magnitudes in absolute magnitude and 6–8 magnitudes (200–1000×) in the other properties, this dictates a sample of 200–250 galaxies to cover the $\sim$80 cells. We find that the combination of the ANGST sample (69 galaxies) with the restricted 11HUGS subsample (189 galaxies with $|b|\geq 30°$ and $B \leq 15.5$) achieves this objective while providing excellent coverage of SFRs, absolute magnitudes, and infrared properties (see Figs 1–2).

Imposing more restrictive cuts in either distance, apparent magnitude, or Galactic latitude compromises this physical sampling with a large cost in galaxies lost per hour saved in observing time. And the other alternative of identifying a smaller subsample based on pre-determined physical properties would defeat the central purpose of an unbiased volume-limited survey. 38 of the sample galaxies have already been observed with SINGS, and we have designed our observing strategy to allow these galaxies to be smoothly integrated into the *LVL* sample.

## 2.2 IRAC Imaging

The IRAC observing strategy follows that of SINGS, which shows that stellar and small grain dust emission is typically detected out to the optical radius at a surface brightness level of $\sim$0.04 MJy sr$^{-1}$ (Regan et al. 2006; Dale et al. 2000). For reference all 75 SINGS galaxies, including several M81 dwarfs, were detected in the stellar-dominated 3.6 and 4.5 $\mu$m bands (the faintest galaxy, M81 dwA with $B = 16.5$ and no star formation at any wavelength, was a $2\sigma$ detection; Dale et al. 2005). We do not expect to detect 8.0 $\mu$m PAH emission in all of the galaxies, but will place meaningful limits in those cases.

For galaxies smaller than the IRAC field of view ($D_{25} \leq 300''$) we have constructed AORs using four dithered 30 s integrations. For larger galaxies we use a mosaicking strategy with $\sim$half-array spatial offsets. The sizes of the mosaic 'cores' have been tailored to the optical size of each galaxy. Two sets of IRAC maps will be obtained for each source to enable asteroid removal and map redundancy. The net exposure time per pixel thus is 240 s (120 s around the $\sim 2'.5$-wide mosaic peripheries). Since we will be observing each source in all IRAC channels, ample sky coverage will automatically be provided by the non-overlapping nature of the two IRAC imagers. The high dynamic range option (additional $\sim$1 s exposures) will be employed to allow us to recover information in cases where bright sources would saturate the detector in 30 s. The required integration times for each target are listed in Section 7. The total time required is 87.2 hours for 183 targets.

## 2.3 MIPS Imaging (Cold MIPS AORs)

Galaxies will be imaged in all 3 MIPS bands, using the highly successful scan mapping strategy employed by SINGS. The scan mode is used even on galaxies small enough to fit within the array FOV, because achieving adequate background measurements for extended targets in photometry mode is less efficient than the scan mode. Each map will be performed at the medium scan rate, and will include multiple scan legs tailored to the size of the galaxy and half-array offsets between scan legs. Each galaxy will be mapped twice, with the maps separated by 10–40 days to allow time for asteroids to move out of the field. This second map will be performed in the reverse direction (the "backward mapping" mode), with offsets in the cross-scan and in-scan directions. Taken together, these mapping strategies ensure that each point on the galaxy is scanned over in two different directions, which aids reduction of array artifacts on both Si:As and Ge:Ga arrays. The in-scan offset ensures that Ge:Ga stimflashes do not occur at the same point in both maps and thereby improves the calibration. The integration time per point and expected $1\sigma$ low-background surface-brightness sensitivity (using the SENS-PET tool on the SSC website) is 160, 80, and 16 seconds and 0.059, 0.32, and 0.85 MJy/sr at 24, 70, and 160 $\mu$m, respectively. The required integration times for each target are listed in Section 7. The total time required is 193.3 hours for 205 targets. *This program requires cold MIPS campaigns.*

With this observing strategy, we expect to detect most galaxies brighter than $B$ =15–16. Above $B \sim 14.3$, every galaxy in the SINGS sample and every galaxy in the MIPS starburst GTO sample (PID 59, which uses a similar observing strategy) is detected in all 3 MIPS bands. For fainter objects ($B$ =14.5–18) the detection rate in those combined samples falls to 50% (3 of 6). We considered several strategies to predict which galaxies would be undetectable with MIPS, including sample cuts in apparent and absolute magnitude and SFR. In every instance we could point to counterexamples where Spitzer would almost certainly detect some galaxies which fell below these putative selection limits. Consequently we have chosen to maintain the unbiased nature of the survey and seek to obtain IRAC and MIPS imaging for all of the targets. We estimate that up to 25 of the 204 MIPS targets may be undetected by MIPS in at least the 160$\mu$m band, via standard reductions (the problem is predicting which!), and for those we will employ smoothing and image stacking strategies to derive rigorous and physically meaningful upper limit fluxes.

## 2.4 IRAC and MIPS Data Processing

The multi-epoch, multiple-pointing IRAC observations for each galaxy will be combined into one single mosaic for each band, using techniques and software developed and extensively tested for the SINGS Legacy project. The final images will be created using the SSC–produced Basic Calibrated Data as a starting point. For each frame, distortion corrections, rotations (if multiple epochs are present), bias structure and bias-drift corrections will be applied. Image offsets between the frames forming a mosaic are determined using cross-correlation algorithms simultaneously in all four bands, with expected accuracies of 0.1–0.2 pixels. Cosmic rays will be rejected using standard drizzle methods, while asteroids will be removed from the comparison of multi-epoch images. The drizzle packages will also be used to produce the final mosaics with a 0.75 arcsec pixel size and maximal resolution.

The MIPS scan maps will be reduced and mosaicked with the MIPS Data Analysis Tool (DAT; Gordon et al. 2005) supplemented with custom reduction scripts written specifically to improve the MIPS reductions of resolved galaxies. This method of reduction was used for all the SINGS galaxies as well as very large MIPS/GTO galaxies (M31, M33, M101, etc.). The custom reduction scripts include extra steps beyond that of the MIPS DAT. At 24 $\mu$m, the extra steps include readout offset correction, array averaged background subtraction, and exclusion of the first five images in each scan leg due to boost frame transients. At 70 and 160 $\mu$m, the extra processing step is a pixel-dependent background subtraction for each map to remove residual detector drifts and background cirrus and zodiacal emissions.

## 2.5 Organization of Data Processing and Project

Our team draws from the 11HUGS and ANGST projects as well as a core set of members of the Spitzer SINGS Legacy project. The IRAC and MIPS data processing will be carried out by SINGS team members who managed those respective processing efforts for SINGS.

As PI Kennicutt will be responsible for overall scientific direction and management of the project. Engelbracht will serve as Technical Contact with lead responsibility for the Spitzer observations, and Calzetti will supervise the data product deliveries, duplicating their roles with the SINGS project. Lee will serve as Deputy PI and coordinator for the scientific activities. Kennicutt, Lee, Calzetti, Engelbracht, and Dalcanton will serve as the management group for the project, and will meet regularly by telecon to coordinate activities and schedules. Other key responsibilities will be filled by Calzetti and Dale (IRAC processing), Gordon and Engelbracht (MIPS processing), and Sakai (data product validation and documentation). Ancillary data will be handled by Gil de Paz (UV), Lee (H$\alpha$ and broadband), Williams, Skillman, and Dalcanton (HST), van Zee, Walter, and Begum (radio).

# 3 Legacy Data Products Plan

Our team has extensive experience in Legacy data deliveries from the SINGS project (4 deliveries to date, with the last scheduled for April). Image product definitions, processing steps, and documentation will be adapted directly from SINGS.

• IRAC Data Products

For each galaxy the final IRAC data products will be four astrometrically aligned images (one image for each band), each as a single extension FITS file, calibrated in MJy/sr and with a pixel size of 0.75” and standard WCS protocols. Trimmed image mosaics will be delivered with standard convention North up, East left, and will be background–subtracted.

• MIPS Data Products

The MIPS images will be delivered as single-extension FITS files, one for each of the 24, 70, and 160 $\mu$m bands, with pixel sizes of 1.5, 4.5, and 9.0 arcsec respectively. The images will be calibrated in MJy/sr, with a fixed background removed. Images from the large scans will be cropped to cover the galaxies along with sufficient surrounding regions to facilitate variable background (e.g., cirrus) removal. Otherwise image formatting and astrometry will be done in the same way as for the IRAC products.

• Ancillary Data Products

H$\alpha$ and $R$-band images have been obtained for most galaxies in the sample. These images will be delivered following the same procedures as the SINGS DR4 H$\alpha$ images. Processed GALEX NUV and FUV images are being produced as part of the 11HUGS project and will be delivered to MAST (e.g., broadly following Gil de Paz et al. 2007). GALEX time to observe 20 ANGST galaxies not in the original 11HUGS sample has been approved. As an approved HST Treasury Project ANGST will provide reduced imaging and color-magnitude data for all of the galaxies in the sample. A corollary HST archival project, the Archive of Nearby Galaxies (ANGRRR), will supplement this with state-of-the-art reduction of ACS and WFPC2 imaging of other galaxies in the sample.

Several other observing programs are under way to extend the multi-wavelength coverage of this dataset. None of these constitutes a formal Legacy deliverable, but as was our experience with SINGS, we expect that many of these complementary data products will be released over the lifetime of the project. High-resolution VLA aperture synthesis maps (HI and continuum) for about half of the sample are available either from the VLA THINGS survey (F. Walter, PI), a new ANGST follow-up survey (J. Ott, PI), a GMRT survey of nearby dIrr galaxies (A. Begum, PI), and other archival sources. Likewise we are assembling and obtaining groundbased $UBVI$ imaging for the sample, and these will be integrated into the multi-wavelength data collection. Finally integrated driftscan spectra for more than half of the 11HUGS galaxies have been obtained (Moustakas & Kennicutt 2006 and new data), and will provide independent metallicity and reddening information.

• Delivery Schedule

We aim to follow the practice of the SINGS project and deliver all images in three 6-month increments, providing an adequate flow of observations and BCD data. Although the imaging dataset here is 2.5 times larger than SINGS, we believe that the combination of mature data pipelines and accumulated experience should allow us to meet this schedule (for the last two SINGS deliveries all 75 image datasets were reprocessed each time).

# 4 Figures and Tables

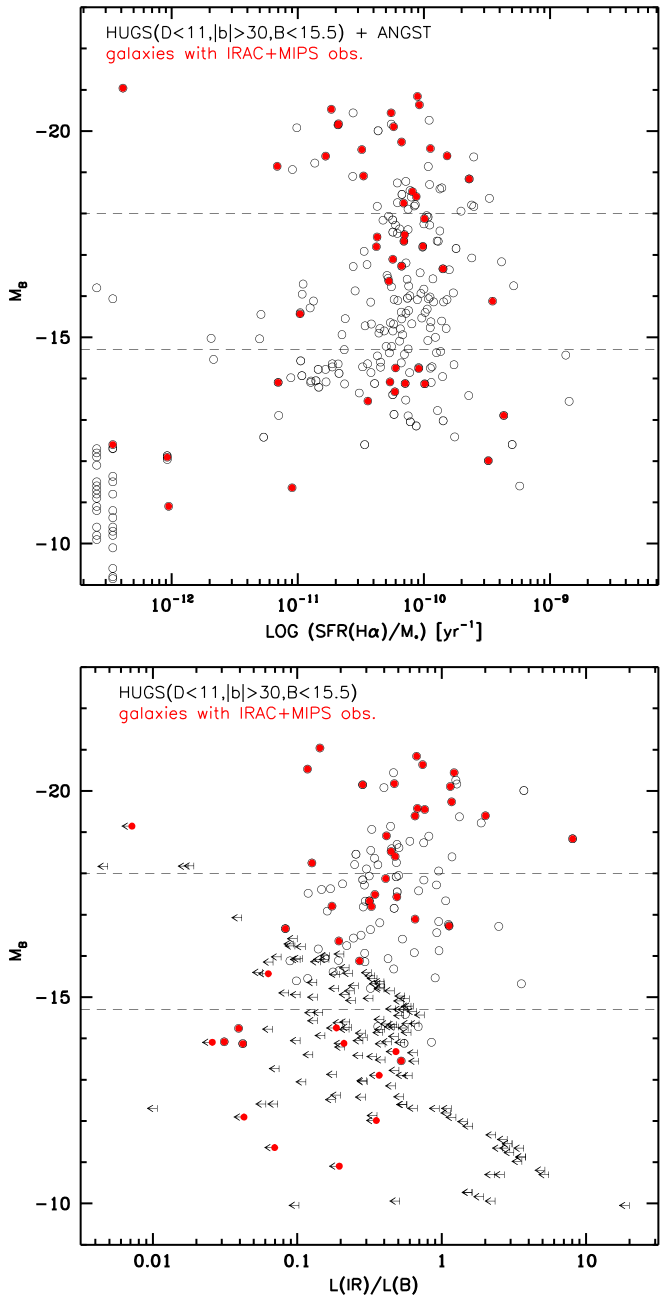


**Figure 1:** Top: *Distribution of Hα star formation rate per unit mass vs absolute blue magnitude*, for galaxies within 11 Mpc. Filled (red) points indicate galaxies with IRAC and MIPS observations, while the open circles denote galaxies to be added by our *Local Volume Legacy* survey. Note the wide range of SFRs (logarithmic scale), even among galaxies of fixed luminosity. Points along the lower left edge of the plot include ANGST dSph galaxies, and a few (mainly ANGST) dIrr galaxies without Hα data at present. Most of the latter show recent star formation, based on their CMDs.
Bottom: *Distribution of IRAS infrared/blue luminosity ratios vs absolute magnitude* for the same galaxies. Again filled (red) points denote galaxies observed by Spitzer, with proposed targets indicated with open circles or arrows. Lines with arrows designate galaxies not detected with IRAS, with corresponding 3-$\sigma$ upper limits in $L_{IR}/L_B$ indicated). This proposal would produce IRAC and MIPS imaging for *all* of the galaxies plotted.

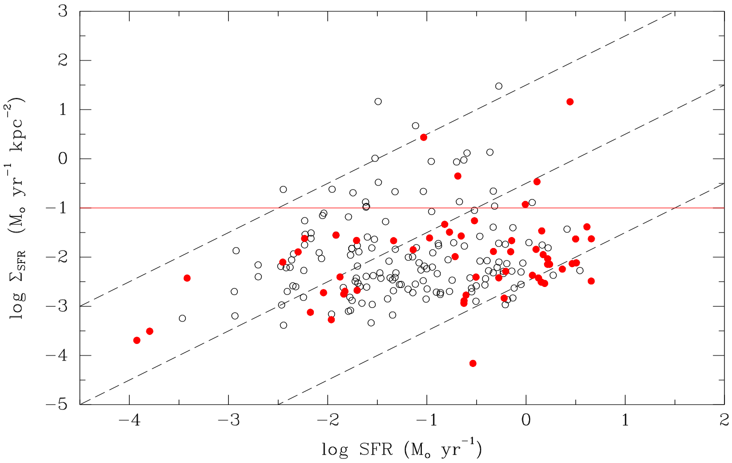


**Figure 2:** *Total star formation rate vs SFR intensity* (SFR per unit area) for the proposed sample galaxies (open circle) and for galaxies with existing IRAC and MIPS observations (red points). Dashed diagonal lines denote loci of constant galaxy radii, from 0.1 kpc (top), 1 kpc (middle) to 10 kpc (bottom). The proposed sample greatly increases the coverage in this diagram, most notably for starburst galaxies with 0.1 $M_\odot$ yr$^{-1}$ kpc$^{-2}$ (indicated by the solid horizontal line).

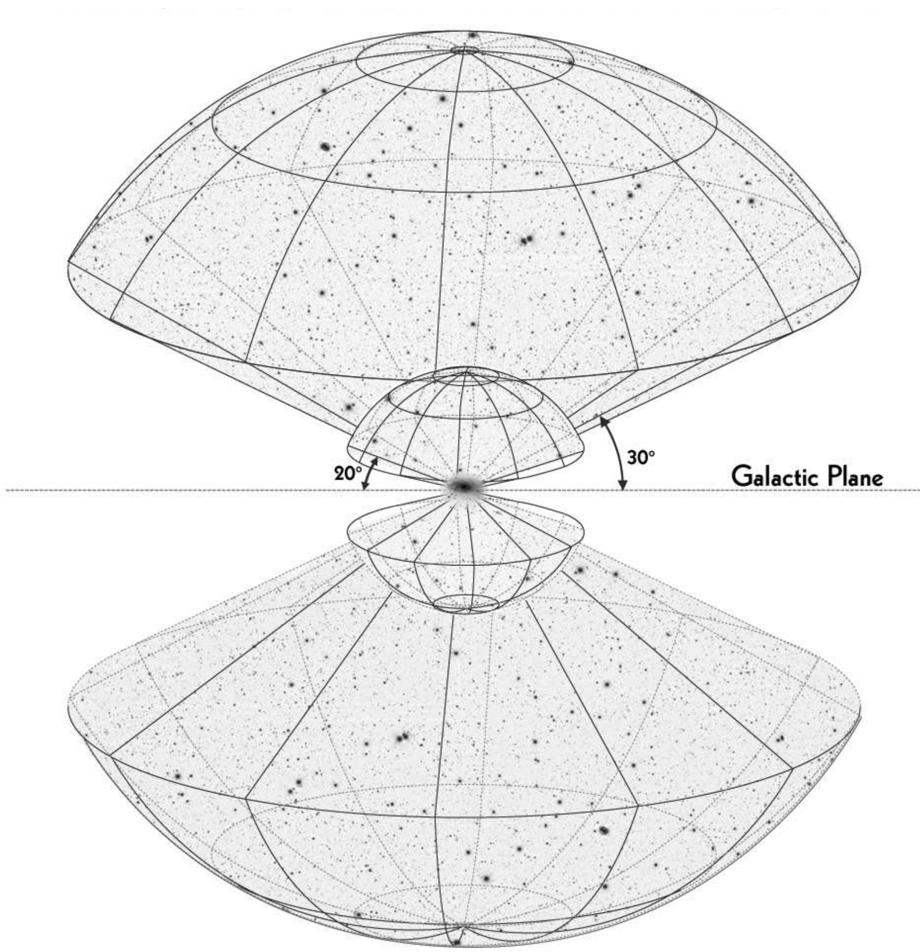


**Figure 3:** *The volume limits of our proposed sample.* The tiered observing strategy includes (1) *all* known galaxies in the inner cones, which begin beyond the Local Group and extend to 3.5 Mpc, and (2) magnitude-limited coverage to B=15.5 mag within the outer cones, which span between 3.5 and 11 Mpc. Graphic credit: Pete Marenfeld (NOAO/AURA/NSF)

# 4 References

Calzetti, D. et al. 2005, ApJ, 633, 871
Cannon, J.M. et al. 2005, ApJ, 630, L37
Cannon, J.M. et al. 2006a, ApJ, 647, 293
Cannon, J.M. et al. 2006b, ApJ, 652, 1170
Daddi, E. et al. 2005, ApJ, 631, L13
Dale, D.A. et al. 2000, AJ, 120, 583
Dale, D.A. et al. 2005, ApJ, 633, 857
Dale, D.A. et al. 2007, ApJ, 655, 863
Dohm-Palmer, R. 1997, AJ, 114, 2527
Engelbracht, C.W. et al. 2005, ApJ, 628, L29
Förster-Schreiber, N.M. et al. 2004, A&A, 419, 501
Gil de Paz, A. et al. 2007, ApJS, in press (astro-ph/0606440)
Gordon, K. D. et al. 2005, PASP, 117, 503
Houck, J.R. et al. 2004, ApJS, 154, 211
Kennicutt, R.C. 1998, ARAA, 36, 189
Kennicutt, R.C. et al. 2003, PASP, 115, 928
Kennicutt, R.C. et al. 2005, in *Starbursts - From 30 Doradus to Lyman-break Galaxies*, eds. R de Grijs, R. M. González Delgado, Astrophysics & Space Science Library, Vol. 329, p187
Kennicutt, R.C. 2007a, in Infrared Diagnostics of Galaxy Evolution, ASP Conf Ser, in press
Kennicutt, R.C. et al. 2007b, ApJ, submitted
Lee, J.C. 2006, PhD thesis, University of Arizona
Madden, S.C. et al. 2006, A&A, in press (astro-ph/0510086)
Moustakas, J., & Kennicutt, R.C. 2006, ApJS, 164, 81
Noeske, K.G. et al. 2005, A&A, 429, 115
Regan, M. et al. 2006, ApJ, 652, 1112
Rosenberg, J.L. et al. 2006, ApJ, 636, 742
Roussel, H. et al. 2001, A&A, 372, 406
Ryan-Weber, E. et al. 2002, AJ, 124, 1954
Valiante, E. et al. 2007, ApJ, in press (astro-ph/0701816)
Walter, F. et al. 2007, ApJ, in press (astro-ph/0702378)
Wu, Y. et al. 2006, ApJ, 639, 157
Yan, L. 2005, NewAR, 49, 420

# 5 Brief Resume/Bibliography

**Robert Kennicutt**, the PI, is the Plumian Professor at the University of Cambridge, and Professor/Astronomer at Steward Observatory. He has written >150 papers on star formation and the ISM in nearby galaxies, and is PI of the SINGS Legacy project.

**Ayesha Begum** (Cambridge) is a postdoctoral research associate at the IoA, working on observations of gas and star formation in spiral and dwarf galaxies.

**Daniela Calzetti** (UMass) is Deputy PI of SINGS and one of the world's leading experts on star formation and dust in galaxies.

**Julianne Dalcanton** (Washington) is an expert on galactic structure and evolution, and PI of the HST ANGST Treasury project and ANGRRR Archival Legacy program.

**Danny Dale** (Wyoming) is a member of the SINGS team and an expert on the infrared properties of galaxies.

**Chad Engelbracht** (Arizona) is the Instrument Scientist for MIPS, a member and technical contact for the SINGS project, and an expert on IR properties of starbursts.

**Jose Funes, S.J.** (Vatican Obs) is Director of the Vatican Observatory, and a member of the 11HUGS team.

**Armando Gil de Paz** (Madrid) is a member of the GALEX science team and the 11HUGS team, and an expert on star-forming spiral and dwarf galaxies.

**Karl Gordon** (Arizona) is a member of the SINGS team and the MIPS GTO team, and a leading expert on dust in galaxies.

**Benjamin Johnson** (Columbia) is completing his Ph.D. on multi-wavelength observations of galaxies, and will move to the IoA as a postdoc this fall.

**Janice Lee** (NOAO/Carnegie) is a Hubble Fellow at NOAO, and wrote her PhD dissertation on the star formation burst properties of dwarf galaxies using the 11HUGS sample.

**Shoko Sakai** (UCLA) is a member of the 11HUGS team and is leading an H$\alpha$ imaging survey of nearby Abell clusters.

**Evan Skillman** (Minnesota) is an expert on the evolution of dwarf galaxies, and a member of the ANGST team.

**Liese van Zee** (Indiana) is a member of the 11HUGS team and an expert on the ISM and star formation properties of dwarf galaxies.

**Fabian Walter** (MPIA) is an expert on the ISM in galaxies. He leads the SINGS subgroup on dwarf galaxies, and is PI of the VLA HI Nearby Galaxy Survey (THINGS).

**Daniel Weisz** (Minnesota) is completing a thesis on star formation histories of galaxies from ANGST.

**Benjamin Williams** (Washington) is an expert on resolved stellar populations, clusters, and x-ray sources in nearby galaxies, and the lead postdoc of the ANGST team.

**Yanling Wu** is a Ph.D. student at Cornell and a member of the IRS GTO team, working under the direction of Jim Houck on the infrared properties of dwarf galaxies.

**Relevant Publications** (space limited)

*SINGS: The SIRTF Nearby Galaxies Survey*, R.C. Kennicutt et al. 2003, PASP, 115, 928

*Star Formation in Galaxies Along the Hubble Sequence*, R.C. Kennicutt 1998, ARAA, 36, 189

*An Ultraviolet-to-Radio Broadband Spectral Atlas of Nearby Galaxies*, D.A. Dale et al. 2007, ApJ, 655, 863

*Star Formation in NGC 5194 (M51a): The Panchromatic View from GALEX to Spitzer*, D. Calzetti et al. 2005, ApJ, 633, 871

# 6 Observation Summary Table

**Local Volume Legacy Observation Request Overview**

| Instrument | Bands [$\mu$m] | Coverage | $3\sigma$ Sensitivity [MJy sr$^{-1}$] | Galaxies | Time [hrs] |
|---|---|---|---|---|---|
| IRAC | 3.6 | $> D_{25}$ | 0.02 | 183 | 87.2 |
| | 4.5 | $> D_{25}$ | 0.02 | | |
| | 5.8 | $> D_{25}$ | 0.11 | | |
| | 8.0 | $> D_{25}$ | 0.11 | | |
| MIPS | 24 | $> D_{25}$ | 0.2 | 205 | 193.3 |
| | 70 | $> D_{25}$ | 0.9 | | |
| | 160 | $> D_{25}$ | 1.7 | | |
| | | | | TOTAL | **280.5 hrs** |

The table below lists all 258 galaxies in the *LVL* sample, including objects for which the necessary IRAC and/or MIPS observations are already available. The requested IRAC and MIPS AOR times for each target are shown. Blank time entries are given for galaxies that have sufficient quality data in the archives and do not need to be observed.

**Local Volume Legacy Sample**

| Galaxy Name | RA (J2000) DEC | $D_{25}$ [′] | IRAC [s] | MIPS [s] | Duplication |
|---|---|---|---|---|---|
| WLM | 000158.1-152739 | 11.5 | — | — | |
| NGC0024 | 000956.7-245744 | 5.8 | — | — | |
| NGC0045 | 001404.0-231055 | 8.5 | 4835 | 5509 | |
| NGC0055 | 001454.0-391149 | 32.4 | — | — | |
| NGC059 | 001525.4-212642 | 2.6 | 1129 | 3494 | X |
| ESO410-G005 | 001531.4-321047 | 1.3 | 1129 | 2487 | |
| Sculptor-dE1 | 002351.7-244218 | 0.9 | 1129 | 2487 | |
| ESO294-G010 | 002633.4-415119 | 1.1 | 1129 | 2487 | |
| IC1574 | 004303.8-221449 | 2.1 | 1129 | 2487 | |
| NGC0247 | 004708.3-204538 | 21.4 | 13506 | 10546 | |
| NGC0253 | 004733.1-251718 | 27.5 | — | 13568 | X |
| ESO540-G030 | 004920.9-180432 | 1.2 | 1129 | 2487 | |
| UGCA015 | 004949.2-210054 | 1.7 | 1129 | 2487 | |
| ESO540-G032 | 005024.3-195424 | 1.3 | 1129 | 2487 | |
| UGC00521 | 005112.2+120131 | 0.9 | 1129 | 2487 | |
| SMC | 005244.8-724943 | 316.2 | — | — | |
| NGC0300 | 005453.5-374100 | 21.9 | 11424 | 10546 | X |
| UGC00668 | 010447.8+020704 | 16.2 | — | — | |
| UGC00685 | 010722.4+164102 | 1.2 | 1129 | 2487 | |
| UGC00695 | 010746.4+010349 | 1.1 | 1129 | 2487 | |

**Local Volume Legacy Sample**

| Galaxy Name | RA (J2000) DEC | $D_{25}$ [′] | IRAC [s] | MIPS [s] | Duplication |
|---|---|---|---|---|---|
| NGC404 | 010927.0+354304 | 2.5 | — | 2487 | |
| UGC00891 | 012118.9+122443 | 2.3 | 1129 | 2487 | |
| UGC01056 | 012847.3+164119 | 0.9 | 1129 | 2487 | |
| UGC01104 | 013242.5+181902 | 1.0 | 1129 | 2487 | |
| NGC0598 | 013350.9+303937 | 70.8 | — | — | |
| NGC0625 | 013504.2-412615 | 5.8 | 2638 | 4502 | |
| NGC0628 | 013641.7+154659 | 10.5 | — | — | |
| UGC01176 | 014009.9+155417 | 4.6 | 1129 | 3494 | |
| ESO245-G005 | 014503.7-433553 | 3.6 | 1129 | 3494 | |
| UGC01249 | 014730.6+271952 | 6.9 | 3184 | 4502 | |
| NGC0672 | 014754.3+272559 | 7.2 | 2638 | 4502 | |
| ESO245-G007 | 015106.3-442641 | 4.9 | 1129 | — | X |
| NGC0784 | 020117.0+285015 | 6.6 | 3184 | 4502 | |
| NGC855 | 021403.6+275238 | 2.6 | — | — | |
| ESO115-G021 | 023748.1-612018 | 4.9 | 1129 | 3494 | |
| ESO154-G023 | 025650.4-543417 | 8.5 | 3643 | 5509 | |
| NGC1291 | 031718.3-410628 | 9.8 | — | — | |
| NGC1313 | 031815.8-662953 | 9.1 | 4290 | 5509 | |
| NGC1311 | 032007.4-521107 | 3.0 | 1129 | 3494 | |
| UGC02716 | 032407.2+174512 | 1.6 | 1129 | 2487 | |
| IC1959 | 033311.8-502438 | 2.8 | 1129 | 3494 | |
| NGC1487 | 035546.1-422205 | 3.3 | 1129 | 3494 | |
| NGC1510 | 040332.6-432400 | 1.3 | 1129 | 2487 | |
| NGC1512 | 040354.3-432057 | 8.9 | — | — | |
| NGC1522 | 040607.7-524009 | 1.2 | 1129 | 2487 | |
| IC2049 | 041204.3-583325 | 1.0 | 1129 | 2487 | |
| ESO483-G013 | 041241.3-230936 | 1.6 | 1129 | 2487 | |
| ESO158-G003 | 044616.7-572035 | 1.6 | 1129 | 2487 | |
| ESO119-G016 | 045129.2-613903 | 2.3 | 1129 | 2487 | |
| NGC1705 | 045413.7-532141 | 1.9 | — | — | |
| NGC1744 | 045957.6-260119 | 8.1 | 3643 | 5509 | |
| NGC1796 | 050242.8-610823 | 1.9 | 1129 | 2487 | |
| ESO486-G021 | 050319.7-252523 | 1.2 | 1129 | 2487 | |
| MCG-05-13-004 | 050624.1-315711 | 0.2 | 1129 | 2487 | |
| NGC1800 | 050625.4-315715 | 2.0 | 1129 | 2487 | |
| UGCA106 | 051159.3-325821 | 3.5 | 1129 | 3494 | |
| LMC | 052334.5-694522 | 645.7 | — | — | |
| kkh037 | 064745.8+800726 | 1.2 | 1129 | 2487 | |
| NGC2366 | 072854.6+691257 | 7.3 | 3004 | 4502 | |
| UGCA133 | 073411.4+665310 | 3.0 | 1129 | 3495 | |
| NGC2403 | 073651.4+653609 | 21.9 | — | — | |
| NGC2500 | 080153.3+504415 | 2.9 | — | 3494 | X |

**Local Volume Legacy Sample**

| Galaxy Name | RA (J2000) DEC | $D_{25}$ [′] | IRAC [s] | MIPS [s] | Duplication |
|---|---|---|---|---|---|
| NGC2537 | 081314.7+455926 | 1.7 | — | 2487 | X |
| UGC04278 | 081358.9+454434 | 4.7 | — | — | |
| UGC04305 | 081904.0+704309 | 7.9 | — | — | |
| NGC2552 | 081920.1+500025 | 3.5 | 1129 | 3494 | |
| M81dwA | 082356.0+710145 | 1.3 | — | — | |
| UGC04426 | 082828.4+415124 | 2.0 | 1129 | 2487 | |
| UGC04459 | 083407.2+661054 | 1.5 | — | — | |
| UGC04483 | 083703.0+694631 | 1.1 | — | 2487 | X |
| NGC2683 | 085241.4+332514 | 9.3 | 4290 | 5509 | |
| UGC04704 | 085900.3+391236 | 4.1 | 1129 | 3494 | |
| UGC04787 | 090734.9+331636 | 2.1 | 1129 | 2487 | |
| UGC04998 | 092512.1+682259 | 1.6 | 1129 | 2487 | |
| NGC2903 | 093210.1+213004 | 12.6 | 5558 | 7524 | X |
| UGC05076 | 093236.4+515219 | 1.0 | 1129 | 2487 | |
| CGCG035-007 | 093444.9+062532 | 0.8 | 1129 | 2487 | |
| UGC05139 | 094032.3+711056 | 3.6 | — | — | |
| IC0559 | 094443.9+093655 | 0.8 | 1129 | 2487 | |
| F8D1 | 094447.1+672619 | 5.5 | 2638 | 4502 | |
| [FM2000]1 | 094510.0+684554 | 0.9 | 1129 | 2487 | |
| NGC2976 | 094715.3+675500 | 5.9 | — | — | |
| LEDA166101 | 095010.5+673024 | 2.4 | 1129 | 2487 | |
| UGC05272 | 095022.4+312916 | 2.1 | 1129 | 2487 | |
| UGC05288 | 095117.0+074939 | 1.3 | 1129 | 2487 | |
| BK03N | 095348.5+685808 | 0.5 | 1129 | 2487 | |
| NGC3031 | 095533.2+690355 | 26.9 | — | — | |
| NGC3034 | 095552.2+694047 | 11.2 | — | — | |
| UGC05340 | 095645.7+284935 | 2.7 | — | 3494 | |
| KDG061 | 095703.1+683531 | 1.2 | 1129 | 2487 | |
| UGC05336 | 095732.0+690245 | 2.5 | 1129 | 2487 | |
| Arp'sLoop | 095732.6+691700 | 1.8 | 1129 | 2487 | |
| UGC05364 | 095926.4+304447 | 5.1 | 2085 | — | X |
| UGC05373 | 100000.1+051956 | 5.1 | 2638 | — | X |
| kkh057 | 100015.9+631106 | 0.6 | 1129 | 2487 | |
| UGCA193 | 100236.0-060049 | 2.8 | 1129 | 3494 | |
| NGC3109 | 100306.6-260932 | 17.0 | 9500 | 9539 | |
| NGC3077 | 100320.6+684404 | 5.4 | 3184 | 4502 | X |
| AM1001-270 | 100403.9-271955 | 2.0 | 1129 | — | |
| BK05N | 100441.1+681522 | 0.8 | 1129 | 2487 | |
| UGC5428 | 100506.4+663332 | 1.7 | 1129 | 2487 | |
| UGC05423 | 100530.6+702152 | 0.9 | — | — | |

**Local Volume Legacy Sample**

| Galaxy Name | RA (J2000) DEC | $D_{25}$ [′] | IRAC [s] | MIPS [s] | Duplication |
|---|---|---|---|---|---|
| UGC5442 | 100701.9+674939 | 1.9 | 1129 | 2487 | |
| UGC05456 | 100719.6+102146 | 1.6 | 1129 | 2487 | |
| IKN | 100805.9+682357 | 2.7 | 1129 | 3495 | |
| SextansA | 101100.8-044134 | 5.9 | — | — | |
| [HS98]117 | 102125.2+710651 | 1.5 | 1129 | 2487 | |
| NGC3239 | 102505.6+170937 | 5.0 | 1129 | 3494 | |
| DDO078 | 102627.4+673916 | 2.0 | 1129 | 2487 | |
| UGC05672 | 102820.9+223417 | 1.8 | 1129 | 2487 | |
| UGC05666 | 102821.2+682443 | 13.2 | — | — | |
| UGC05692 | 103035.0+703707 | 3.2 | 1129 | 3494 | |
| NGC3274 | 103217.1+274007 | 2.1 | 1129 | 2487 | |
| BK06N | 103429.8+660030 | 1.1 | 1129 | 2487 | |
| NGC3299 | 103623.8+124227 | 2.2 | 1129 | 2487 | |
| UGC05764 | 103643.3+313248 | 2.0 | 1129 | 2487 | |
| UGC05797 | 103925.2+014305 | 1.0 | 1129 | 2487 | |
| UGC05829 | 104242.2+342656 | 4.7 | 1129 | 3494 | |
| NGC3344 | 104330.9+245522 | 7.1 | — | 4502 | X |
| NGC3351 | 104357.8+114214 | 7.4 | — | — | |
| NGC3368 | 104645.7+114912 | 7.6 | — | 5509 | X |
| UGC05889 | 104722.3+140410 | 2.2 | 1129 | 2487 | |
| UGC05923 | 104907.6+065502 | 0.9 | — | 2487 | |
| UGC05918 | 104936.5+653150 | 2.4 | 1129 | 2487 | |
| NGC3432 | 105231.3+363711 | 6.8 | 3184 | 4502 | |
| KDG73 | 105257.1+693258 | 0.6 | 1129 | 2487 | |
| NGC3486 | 110023.9+285830 | 7.1 | — | 4502 | X |
| NGC3510 | 110343.4+285313 | 4.0 | 1129 | 3494 | |
| NGC3521 | 110548.6-000209 | 11.0 | — | — | |
| NGC3593 | 111437.0+124904 | 5.2 | — | 4502 | X |
| NGC3623 | 111855.9+130537 | 9.8 | 4290 | 5509 | |
| NGC3627 | 112015.0+125930 | 9.1 | — | — | |
| NGC3628 | 112016.9+133520 | 14.8 | 6206 | 7524 | X |
| UGC06457 | 112712.2-005941 | 0.9 | 1129 | 2487 | |
| UGC06541 | 113328.9+491414 | 1.2 | — | 2487 | |
| NGC3738 | 113548.8+543126 | 2.5 | — | 2487 | X |
| NGC3741 | 113606.2+451701 | 2.0 | 1129 | 2487 | |
| UGC06782 | 114857.2+235016 | 2.0 | 1129 | 2487 | |
| UGC06817 | 115053.0+385249 | 4.1 | 1129 | 3494 | |
| UGC06900 | 115539.4+313110 | 2.1 | 1129 | 2487 | |
| NGC4020 | 115856.6+302444 | 2.1 | 1129 | 2487 | |
| NGC4068 | 120400.8+523518 | 3.3 | 1129 | 3494 | |
| NGC4080 | 120451.8+265933 | 1.2 | 1129 | 2487 | |

**Local Volume Legacy Sample**

| Galaxy Name | RA (J2000) DEC | $D_{25}$ [′] | IRAC [s] | MIPS [s] | Duplication |
|---|---|---|---|---|---|
| NGC4096 | 120601.0+472840 | 6.6 | 3733 | 4502 | |
| NGC4144 | 120958.4+462727 | 6.0 | — | 4502 | |
| NGC4163 | 121209.1+361009 | 1.8 | 1129 | 2487 | |
| NGC4190 | 121344.7+363803 | 1.7 | 1129 | 2487 | |
| ESO321-G014 | 121349.6-381353 | 1.4 | 1129 | 2487 | |
| UGC07242 | 121408.4+660541 | 2.0 | 1129 | 2487 | |
| UGCA276 | 121457.9+361308 | 1.5 | 1129 | 2487 | |
| UGC07267 | 121523.6+512058 | 2.1 | 1129 | 2487 | |
| NGC4214 | 121538.9+361940 | 8.5 | — | 5509 | X |
| CGCG269-049 | 121546.8+522317 | 1.2 | — | — | |
| NGC4236 | 121642.1+692746 | 21.9 | — | — | |
| NGC4244 | 121729.9+374829 | 16.6 | — | — | |
| NGC4242 | 121730.1+453708 | 5.0 | — | 3494 | X |
| UGC07321 | 121733.8+223226 | 5.5 | — | — | |
| NGC4248 | 121750.3+472431 | 3.0 | 1129 | 3494 | |
| NGC4258 | 121857.5+471814 | 18.6 | — | 9539 | X |
| ISZ399 | 121959.5-172331 | 1.0 | 1129 | 2487 | |
| NGC4288 | 122038.1+461733 | 2.1 | 1129 | 2487 | |
| UGC07408 | 122115.0+454841 | 2.6 | 1129 | 3494 | |
| UGC07490 | 122425.3+702001 | 3.3 | 1129 | 3494 | |
| NGC4395 | 122548.9+333248 | 13.2 | 6206 | 7524 | |
| UGCA281 | 122616.0+482937 | 0.8 | 1129 | 2487 | X |
| UGC07559 | 122705.1+370833 | 3.2 | 1129 | 3494 | |
| UGC07577 | 122740.9+432944 | 4.3 | 1129 | 3494 | |
| NGC4449 | 122811.2+440536 | 6.2 | — | 4502 | X |
| UGC07599 | 122828.5+371401 | 2.0 | 1129 | 2487 | |
| UGC07605 | 122838.7+354303 | 1.1 | 1129 | 2487 | |
| NGC4455 | 122844.1+224921 | 2.8 | 1129 | 3494 | |
| UGC07608 | 122845.3+431335 | 3.4 | 1129 | 3494 | |
| NGC4460 | 122845.5+445151 | 4.0 | — | 3494 | X |
| UGC07639 | 122953.4+473152 | 2.3 | 1129 | 2487 | |
| NGC4485 | 123031.1+414201 | 2.3 | — | 2487 | |
| NGC4490 | 123036.1+413834 | 6.3 | — | 4502 | X |
| UGC07690 | 123226.8+424218 | 1.7 | 1129 | 2487 | |
| UGC07699 | 123248.0+373718 | 3.8 | 1129 | 3494 | |
| UGC07698 | 123254.4+313228 | 6.4 | 2638 | 4502 | |
| UGC07719 | 123400.6+390110 | 1.9 | 1129 | 2487 | |
| UGC07774 | 123622.5+400019 | 3.6 | 1129 | 3494 | |
| UGCA292 | 123840.0+324601 | 1.0 | — | — | |
| MESSIER104 | 123959.4-113723 | 8.7 | — | — | |

**Local Volume Legacy Sample**

| Galaxy Name | RA (J2000) DEC | $D_{25}$ [′] | IRAC [s] | MIPS [s] | Duplication |
|---|---|---|---|---|---|
| NGC4605 | 124000.3+613629 | 5.8 | 2638 | 4502 | |
| NGC4618 | 124132.7+410904 | 4.2 | — | 3494 | X |
| NGC4625 | 124152.6+411626 | 2.2 | — | — | |
| NGC4631 | 124208.0+323226 | 15.5 | — | — | |
| UGC07866 | 124215.1+383012 | 3.4 | 1129 | 3494 | |
| NGC4656 | 124357.7+321005 | 15.1 | 7030 | 8531 | |
| UGC07916 | 124425.1+342312 | 2.5 | 1129 | 2487 | |
| UGC07950 | 124656.4+513646 | 1.3 | 1129 | 2487 | |
| UGC07949 | 124659.8+362835 | 2.0 | 1129 | 2487 | |
| NGC4707 | 124822.9+510953 | 2.2 | 1129 | 2487 | |
| NGC4736 | 125053.0+410714 | 11.2 | — | — | |
| UGC08024 | 125405.2+270855 | 3.0 | — | — | |
| NGC4826 | 125643.7+214052 | 10.0 | — | — | |
| UGC08091 | 125840.4+141303 | 1.1 | 1129 | — | X |
| UGCA319 | 130214.4-171415 | 1.6 | 1129 | 2487 | |
| UGCA320 | 130316.8-172523 | 5.6 | 2085 | 4502 | |
| UGC08188 | 130549.5+373618 | 6.0 | 2638 | 4502 | |
| UGC08201 | 130624.8+674225 | 3.5 | — | — | |
| MCG-03-34-002 | 130756.6-164121 | 0.7 | 1129 | 2487 | |
| UGC08245 | 130834.2+785613 | 1.7 | 1129 | 2487 | |
| NGC5023 | 131212.1+440220 | 6.0 | — | 4502 | |
| CGCG217-018 | 131251.8+403235 | 0.7 | 1129 | 2487 | |
| UGC08313 | 131354.1+421236 | 1.7 | 1129 | 2487 | |
| UGC08320 | 131427.9+455509 | 3.6 | 1129 | 3494 | |
| UGC08331 | 131530.3+472956 | 2.7 | 1129 | 3494 | |
| NGC5055 | 131549.2+420149 | 12.6 | — | — | |
| NGC5068 | 131854.6-210220 | 7.2 | 3733 | 4502 | |
| IC4247 | 132644.4-302145 | 1.3 | 1129 | 2487 | |
| NGC5204 | 132936.2+582506 | 5.0 | — | 3494 | X |
| NGC5194 | 132952.7+471143 | 11.2 | — | — | |
| NGC5195 | 132958.7+471605 | 5.8 | — | — | |
| UGC08508 | 133044.4+545436 | 1.7 | 1129 | 2487 | |
| NGC5229 | 133402.7+475455 | 3.3 | 1129 | 3494 | |
| NGC5238 | 133442.7+513651 | 1.7 | 1129 | 2487 | |
| [KK98]208 | 133635.5-293417 | 6.0 | 2638 | 4502 | |
| NGC5236 | 133700.8-295159 | 12.9 | 6294 | — | X |
| ESO444-G084 | 133720.1-280246 | 1.3 | 1129 | 2487 | |
| UGC08638 | 133919.4+244632 | 1.2 | 1129 | 2487 | |
| UGC08651 | 133953.8+404421 | 2.3 | 1129 | 2487 | |
| NGC5253 | 133955.9-313824 | 5.0 | — | 3494 | X |
| NGC5264 | 134136.9-295450 | 2.5 | 1129 | 2487 | |

**Local Volume Legacy Sample**

| Galaxy Name | RA (J2000) DEC | $D_{25}$ [′] | IRAC [s] | MIPS [s] | Duplication |
|---|---|---|---|---|---|
| UGC08760 | 135050.6+380109 | 2.2 | 1129 | 2487 | |
| kkh086 | 135433.5+041435 | 0.7 | 1129 | 2487 | |
| UGC08837 | 135445.7+535403 | 4.3 | 1129 | 3494 | |
| UGC08833 | 135448.7+355015 | 0.9 | 1129 | 2487 | |
| NGC5457 | 140312.5+542055 | 28.8 | — | — | |
| NGC5474 | 140501.5+533945 | 4.8 | — | — | |
| NGC5477 | 140533.1+542739 | 1.7 | 1129 | — | |
| [KK98]230 | 140710.5+350337 | 0.6 | 1129 | 2487 | |
| UGC09128 | 141556.5+230319 | 1.7 | — | 2487 | X |
| NGC5585 | 141948.2+564346 | 5.8 | — | 4502 | X |
| UGC09240 | 142443.4+443133 | 1.8 | 1129 | 2487 | |
| UGC09405 | 143524.4+571519 | 1.7 | 1129 | 2487 | |
| MRK475 | 143905.4+364821 | 0.4 | 1129 | 2487 | X |
| NGC5832 | 145745.7+714056 | 3.7 | 1129 | 3495 | |
| NGC5949 | 152800.7+644547 | 2.2 | 1129 | 2487 | |
| UGC09992 | 154147.8+671515 | 1.6 | 1129 | 2487 | |
| KKR25 | 161347.9+542216 | 1.1 | 1129 | 2487 | |
| NGC6503 | 174927.1+700840 | 7.1 | — | 4502 | |
| IC4951 | 200931.2-615047 | 2.8 | 1129 | 3494 | |
| DDO210 | 204651.8-125053 | 2.2 | 1129 | — | X |
| IC5052 | 205206.3-691213 | 5.9 | — | 4502 | |
| NGC7064 | 212903.0-524603 | 3.8 | 1129 | 3494 | |
| NGC7090 | 213628.6-543324 | 7.4 | — | 4502 | |
| IC5152 | 220241.9-511744 | 5.2 | — | 4502 | |
| IC5256 | 224945.8-684126 | 1.1 | 1129 | 2487 | |
| UGCA438 | 232627.5-322320 | 1.5 | 1129 | 2487 | X |
| ESO347-G017 | 232656.0-372049 | 1.4 | 1129 | 2487 | |
| UGC12613 | 232836.2+144435 | 5.0 | 1129 | — | X |
| IC5332 | 233427.4-360605 | 7.8 | 3733 | 5509 | |
| NGC7713 | 233615.4-375619 | 4.5 | 1129 | 3494 | |
| UGCA442 | 234345.5-315722 | 3.5 | 1129 | 3494 | |
| kkh098 | 234534.0+384304 | 1.1 | 1129 | 2487 | |
| ESO149-G003 | 235202.8-523440 | 2.2 | 1129 | 2487 | |
| NGC7793 | 235749.7-323530 | 9.3 | — | — | |

# 7 Status of Existing Observing Programs

PI R. Kennicutt is the PI for the SINGS Legacy Program (pid 159, 193). Observations for SINGS are virtually completed, and the team has delivered IRAC and MIPS imaging for all 75 galaxies, and approximately half of the spectroscopic products, with the final delivery of all products scheduled for April 2007. The project has produced 22 refereed papers to date, with several more under review or in final preparation stages.

CoI D. Calzetti is PI for Spitzer proposal 20289, "Dust and Star Formation in Extreme Outer Disks: The Case of M83 (NGC5236)". All data are in hand and being processed. A paper is in preparation.

CoI D. Calzetti is PI for GO program 30753, "Dust and Star Formation in Extreme Outer Disks of Spiral Galaxies." Observations for this Cycle 3 program are in progress.

CoI C. Engelbracht is PI for GO program 20176, "Spectral Energy Distributions of Star-Forming Galaxies, from Low Metallicity to Ultraluminous Infrared Galaxies." Data acquisition is under way, and all available data are reduced.

CoI C. Engelbracht is Technical Contact for SINGS (see above).

CoI C. Engelbracht is Technical Contact for the MIPS GTO starburst program (pid 59). Data are fully obtained and reduced, and have been published (Engelbracht et al. 2005, ApJ, 628, L29), with a second paper in preparation.

CoI C. Engelbracht is Technical Contact for the MIPS large-galaxy IOC test (pid 718). Data from this program are published in Engelbracht et al. 2004, ApJS, 154, 248.

Co-I K. Gordon is the TC of the MIPS ERO program 717 to study M81. Data published in "Spatially Resolved Ultraviolet, H-alpha, Infrared, and Radio Star Formation in M81", Gordon et al. 2004, ApJS, 154, 215.

Co-I K. Gordon is the TC of the MIPS GTO programs 60 and 30244 to study the HII regions in M101. All of the PID:60 data have been obtained and results presented at the Spitzer meetings in Fall 2004 and 2005. A paper discussing the main results of this program is in preparation. The PID:30244 data will be obtained this Spring.

Co-I K. Gordon is the TC of the MIPS GTO programs 99 and 30203 to study M31. The PID:99 data have all been obtained and an analysis of the infrared morphology of M31 published in Gordon et al. 2006, ApJ, 638, L87 and the dust content of the companion galaxy NGC 205 has been published in Marleau, et al. 2006, ApJ, 646, 929. The PID:30203 data should be taken this Summer. Additional papers on comparison of the MIPS images to other wavelength data are in preparation by members a large international collaboration which seeded around the MIPS observations.

Co-I K. Gordon is the PI of the GO-2 program 20146 to study the diffuse interstellar extinction curve in the Spitzer infrared. The final observations for this program have recently been taken and all the data has been reduced. A progress report was presented at the Jan 2006 AAS meeting and the analysis of the full dataset is ongoing.

Co-I E. Skillman is PI of GO-3177, Probing the Neutral to Molecular Transition in the Dwarf Starburst Galaxy NGC 4214. A paper is in preparatoin.

Co-I E. Skillman is PI of GO-20425, Dust at Low Metallicity: MIPS Observations of Local Group Dwarfs. Data are obtained and a paper is in preparation.

Co-I Y. Wu is the TC of IRS GTO program 30172 "Spectral Energy Distribution of Low Metallicity Blue Compact Dwarf Galaxies" and program 30669 "Spitzer/IRS View of Blue Compact Dwarf Galaxies". Data aquisition is under way and the available data have been reduced.

# 8 Proprietary Period Modification

This is a Legacy proposal so we waive all proprietary rights.

# 9 Justification of Duplicate Observations

A search of Leopard shows that 76 of the 258 galaxies in the proposed sample have been observed (or are scheduled to be observed) with IRAC, and 53 with MIPS in its scanning mode. One set of nominal duplications that we request involve three of these galaxies. The first is M83, which has IRAC data on the nuclear region through Rieke et al. (pid 00059) and IRAC data on the galaxy outskirts through Calzetti et al. (pid 20289). The aggregate of these observations only cover 25% of the optical disk and therefore merit additional IRAC observations. Moreover, the Rieke et al. nuclear data are shallow enough that our proposed observations would not constitute an official duplication of the nuclear region.

In addition, there are a handful of galaxies for which IRAC observations exist in only two of the four channels. Because the additional time commitment would be small, and to provide a uniform legacy of data, we propose to simply observe these galaxies in all four channels (and thus obtain duplicates in two channels). The galaxies are: ESO245-G007, UGC12613, UGCA438, DDO210, UGC08091, UGCA281, NGC3109, UGC05373, and UGC05364.

Finally, there are a few galaxies for which observations exist, but they are shallow enough that our proposed IRAC observations would be duplications: MRK475, NGC3628, NGC3077, NGC2903, and NGC0300.

Additional MIPS photometry mode data exist for another 26 galaxies. However, we are requesting time to reobserve all of these objects using the standard SINGS scan mapping algorithm, since photometry mode observations provide adequate spatial coverage and background subtraction only for those objects which are point sources at 70 and 160 $\mu$m. We are proposing one duplication of a galaxy with MIPS scan mapping observations. This is NGC 300, which was observed during IOC, and thus suffers from much higher instrumental noise at 70 $\mu$m, due to the high bias voltage applied at that early time in the mission. These observations should be repeated to provide a homogeneous dataset, and to achieve much better sensitivity at 70 $\mu$m).

All such duplications are flagged in the Observation Summary Table.

# 10 Justification of Targets of Opportunity

There are no ToO observations.

# 11 Justification of Scheduling Constraints

We propose two MIPS visits to each target, separated by 10-40 days, to screen out asteroids and to provide sufficient rotation of the spacecraft between visits to help eliminate detector artifacts (e.g. striping with the Ge detectors). The minimum separation allows several degrees rotation between maps while still allowing both observations to be made in the same MIPS campaign, while the maximum separation ensures that both maps are made in the same observing window.

Likewise we propose two IRAC visits for each target to facilitate asteroid removal. In this case the interval between visits can be shorter (approximately 0.2 – 14 days).

# 12 Data Analysis Funding Distribution

Funding should be allocated to the U.S. based Co-Is as follows. The fractions listed are of the total U.S.-based effort:

Engelbracht (includes Gordon) (35%), Calzetti (15%), Dalcanton (5%), Dale (15%), Lee (5%), Sakai (10%), Skillman (5%), Wu (5%), van Zee (5%).

Note that these proportions of funding do not correspond precisely to levels of effort in all cases. For example as a Hubble Fellow Dr. Lee is ineligible for salary support, so the percentage of funding listed underrepresents her contribution to the project. By the same token the largest allocations have been made to Arizona (Engelbracht and Gordon), U. Mass (Calzetti), and Wyoming (Dale), because major portions of the data processing will be done at these sites, requiring hiring of research assistants (see Section 2.5).

For the purposes of determining overall funding, the non-US investigators (Begum, Gil de Paz, Johnson, Walter) will contribute 20% of the total project work effort (5% each). The PI R. Kennicutt holds salaried appointments both at the University of Arizona and the University of Cambridge, but requests no direct support for this project. He will contribute 10% of the total project effort.

# 13 Financial Contact Information

**U. Arizona** (Engelbracht)
Sherry L. Esham, Interim Director
Sponsored Projects Services
The University of Arizona
P. O. Box 3308
Tucson, AZ 85722-3308
Phone: 520-626-6000
Email: sponsor@email.arizona.edu

**Carnegie Observatories** (Lee)
June Napoco-Soriente
The Carnegie Institution of Washington
1530 P Street, NW
Washington, DC 20005
Phone: 202-939-1129
Email: jnapoco-soriente@ciw.edu

**Cornell** (Wu)
Susan L. Jones
Sr. Grant and Contract Officer
Cornell University
120 Day Hall
Ithaca, NY 14853-2801
Phone: 607-255-2945
Fax: 607-255-5058
http://www.osp.cornell.edu/

**Indiana U.** (van Zee)
Barb Platt
Sponsored Research Services
Office for the Vice President for Research
Carmichael Center, Suite L03
530 East Kirkwood Ave
Indiana University
Bloomington, IN 47408
Phone: 812 855 0516
Fax: 812 855 9943
Email: bplatt@indiana.edu

**U. Massachusetts** (Calzetti)
Carol P. Sprague, Director
Office of Grants and Contract Administration
University of Massachusetts
Research Administration Building
70 Butterfield Terrace
Amherst, MA 01003
email:ogca@research.umass.edu
Phone: 413-545-0698
Fax: 413-545-1202

**U. Minnesota** (Skillman)
Kevin McKoskey, Grants Manager
Sponsored Projects Administration
University of Minnesota
Suite 450, McNamara Alumni Center
200 Oak Street SE
Minneapolis, MN 55455
E-mail: awards@umn.edu
Phone: 612-624-5599
Fax: 612-624-4843

**UCLA** (Sakai)
Barbara Harris-Holdrege
Contract and Grant Officer
UCLA Office of Contract and Grant Administration
BOX 951406, Ste 1200, UCLA Wilshire Cntr
Los Angeles, CA 90095-1406
Phone: 310-794-0179
Fax: 310-794-0631
bharris-holdrege@resadmin.ucla.edu

**U. Washington** (Dalcanton)
Office of Sponsored Programs
University of Washington
Box 354945 (Campus Mail Only)
1100 45th St. NE, Suite 300
Seattle, WA 98105
Email: bharris-holdrege@resadmin.ucla.edu
PhoneL 206-543-4043
Fax : 685-1732
Email: osp@u.washington.edu

Assistant Vice Provost for Research:
Executive Director
Carol Zuiches
Payment Address:
University of Washington
Grant and Contract Accounting
12455 Collections Drive
Chicago, IL 60693

**U. Wyoming** (Dale)
Roger Wilmot, Associate Vice President for Research
1000 East University Avenue, Department 3355
University of Wyoming
Laramie, WY 82071
Tel: 307-766-5320
Email: rwilmot@uwyo.edu